Comparison of results from sprite streamer modeling with spectrophotometric measurements by ISUAL instrument on FORMOSAT-2 satellite

Ningyu Liu,[1] Victor P. Pasko,[1] David H. Burkhardt,[1] Harald U. Frey,[2] Stephen B. Mende,[2] Han-Tzong Su,[3] Alfred B. Chen,[3] Rue-Ron Hsu,[3] Lou-Chuang Lee,[3] Hiroshi Fukunishi,[4] and Yukihiro Takahashi[4]

Received 28 July 2005; revised 3 November 2005; accepted 30 November 2005; published 6 January 2006.

[1] Three intensity ratios of the second positive band system of N_2 to N_2 LBH band system, the first negative band system of N_2^+, and the first positive band system of N_2 are obtained separately from sprite streamer modeling and from measurements by ISUAL instrument on FORMOSAT-2 satellite. The direct comparison between the obtained ratios indicates that in order to explain the ISUAL spectrophotometric data the maximum field driving the emissions of an observed sprite event must be greater than three times of the conventional breakdown threshold field. These findings are consistent with an assumption that most of the observed sprite emissions during initial sprite development originate from localized high field regions associated with tips of sprite streamers. **Citation:** Liu, N., et al. (2006), Comparison of results from sprite streamer modeling with spectrophotometric measurements by ISUAL instrument on FORMOSAT-2 satellite, *Geophys. Res. Lett.*, *33*, L01101, doi:10.1029/2005GL024243.

1. Introduction

[2] Sprites are spectacular luminous discharges, which appear in the altitude range of ~40 to 90 km above thunderstorms [e.g., *Sentman et al.*, 1995]. Remote sensing of emissions from sprites gives insightful knowledge about the energetics of electrons and the driving electric field in sprite discharges [e.g., *Morrill et al.*, 2002]. An amazing variety of the decameter-scale filamentary structures revealed by recent telescopic imaging of sprites [e.g., *Gerken and Inan*, 2002] appear to be in a good agreement with a mechanism based on filamentary gas discharge plasmas called streamers [e.g., *Liu and Pasko*, 2004, 2005]. Related modeling results on characteristics of sprite streamers [*Liu and Pasko*, 2004, 2005] are consistent, in particular, with high speed video studies showing very fast vertical development of sprite streamers [e.g., *Stanley et al.*, 1999] and observations of more frequent branching of sprite streamers at the bottom of the sprite than at the top [e.g., *Gerken and Inan*, 2002].

[3] The recent successful launch of the ISUAL instrument on FORMOSAT-2 satellite [*Chern et al.*, 2003] provides new opportunities for studies of sprite spatial, temporal and spectral properties on a global level. The ISUAL instrument contains a spectrophotometer with six individual photometer channels covering the spectral range from the far ultraviolet (FUV) to the near infrared. The photometers provide a set of intensity data on emissions from the first positive ($1PN_2$) and second positive ($2PN_2$) band systems of N_2, N_2 LBH band system, and the first negative band system of N_2^+ ($1NN_2^+$) [*Chern et al.*, 2003; *Mende et al.*, 2005]. To date, many sprites and other transient luminous events (i.e., elves and halos) have been recorded by the ISUAL instrument [*Mende et al.*, 2005], in particular, providing the first spectrophotometric evidence demonstrating the presence of FUV emissions in the sprite spectrum [*Mende et al.*, 2004a, 2004b; *Frey et al.*, 2004].

[4] The purpose of this paper is to conduct a direct comparison between the modeling results on emissions from sprite streamers and spectrophotometric measurements by the ISUAL instrument on the FORMOSAT-2 Satellite.

2. Problem Formulation

2.1. Description of the Streamer Model and the ISUAL Spectrophotometer

[5] Table 1 summarizes the four emission band systems considered in this study. The data presented in Table 1 are well-known [e.g., *Vallance-Jones*, 1974, p. 119] except for the lifetime and quenching altitude of $a^1\Pi_g$ state of N_2 leading to LBH emissions, the most recent information on which is summarized by *Liu and Pasko* [2005]. As discussed in that paper, streamers advancing in weak electric fields ($E < E_k$, E_k is the conventional breakdown threshold field [*Raizer*, 1991, p. 135]) likely occupy a substantial part of the overall sprite volume, and are responsible for most of the observed sprite emissions. To conduct the comparison, we use the modeling calculations for a sprite streamer propagating in a weak applied electric field at 70 km altitude reported by *Liu and Pasko* [2005] (see Figure 1). The modeled streamer is initiated in a high field region (the maximum field is $\sim 3E_k$, where $E_k \simeq 220$ V/m at 70 km), which is created by an enhancement of the weak applied field around a small conducting sphere with a high potential. The streamer is then allowed to propagate into the weak field region. The longest propagation time of the simulated streamer is 0.53 ms, which is of the same order as the 1–2 ms lifetime of sprite streamer channel luminosity observed

[1]Communications and Space Sciences Laboratory, Pennsylvania State University, University Park, Pennsylvania, USA.
[2]Space Sciences Laboratory, University of California, Berkeley, California, USA.
[3]Department of Physics, National Cheng Kung University, Tainan, Taiwan.
[4]Department of Geophysics, Tohoku University, Sendai, Japan.

0094-8276/06/2005GL024243$05.00

Table 1. Summary of Emissions from Sprites Considered in This Study

Emission Band System	Transition	Excitation Energy Threshold (eV)	Lifetime at 70 km Alt.	Quenching Alt. (km)
$1PN_2$	$N_2(B^3\Pi_g)\rightarrow N_2(A^3\Sigma_u^+)$	~7.35	5.4 μs	~53
$2PN_2$	$N_2(C^3\Pi_u)\rightarrow N_2(B^3\Pi_g)$	~11	50 ns	~30
LBH N_2	$N_2(a^1\Pi_g)\rightarrow N_2(X^1\Sigma_g^+)$	~8.55	14 μs	~77
$1NN_2^+$	$N_2^+(B^2\Sigma_u^+)\rightarrow N_2^+(X^2\Sigma_g^+)$	~18.8	69 ns	~48

recently by a high-speed telescopic imaging system [*Marshall and Inan*, 2005].

[6] The first four channels of ISUAL spectrophotometer are designed to measure LBH, $2PN_2$, $1NN_2^+$ and $1PN_2$ emissions, respectively. Channels 1 and 4 measure broadband signal within the wavelength range 150–280 nm (LBH) and 609–753 nm ($1PN_2$), respectively [*Mende et al.*, 2005]. Channels 2 and 3 measure narrowband signal with center wavelength at 337 ($2PN_2$) and 391.4 ($1NN_2^+$) nm, respectively [*Mende et al.*, 2005]. The response curves of the photometer filters are given by *Mende et al.* [2004a].

2.2. Atmospheric Attenuation

[7] The FUV emissions of N_2 LBH band system suffer from attenuation when traveling through the atmosphere, and a ground-based observer is not able to detect these emissions from sprites due to the strong attenuation by high density atmosphere at low altitudes. In the present study, MOSART code has been utilized to calculate the atmospheric transmittance at wavelengths ≥200 nm [*Cornette et al.*, 1995]. For the transmittance at wavelengths below 200 nm, we use the Lambert's law to account for three major attenuation mechanisms: O_2 and O_3 absorption, and molecular Rayleigh scattering. O_2 absorption is described by the Lambert's law $dI_\lambda/I_\lambda = -N_{O_2}\sigma_{a\lambda}ds$, where I_λ is the monochromatic radiation intensity at wavelength λ, N_{O_2} is the number density of O_2, $\sigma_{a\lambda}$ is the absorption cross-section, and ds is an incremental distance along the path of radiation. By integrating Lambert's law along the path, we obtain $I_\lambda(s) = I_\lambda(0)\exp(-\int_0^s N_{O_2}\sigma_{a\lambda}ds')$. Knowing the number density of O_2 and its cross-section data, the monochromatic transmittance is calculated as $I_\lambda(s)/I_\lambda(0) = e^{-u(s)}$, where $u(s)$ is the optical path length, defined as $u(s) = \int_0^s N_{O_2}\sigma_{a\lambda}ds'$. Figure 2a shows O_2 absorption cross-sections over FUV region [e.g., *Yoshino et al.*, 1992; *Minschwaner et al.*, 1992; *Amoruso et al.*, 1996; *Yoshino et al.*, 2005]. From the expression of $u(s)$, it can be seen that optical path length depends on the integrated O_2 number density along the path. For the simple geometry illustrated by Figure 2b, the transmittance varies with the respective altitudes of the sprite h_s and satellite h_r, and the distance s between them. If the altitude of a point P on the path of the radiation is represented by h, we have $\cos\theta = \frac{(h_s+R_E)^2+s^2-(h_r+R_E)^2}{2(h_s+R_E)s}$, where θ is shown in Figure 2b, R_E is the radius of the Earth, and $h = \sqrt{(h_s+R_E)^2+s'^2-2(h_s+R_E)s'\cos\theta} - R_E$, i.e., $h = h(s')$. Assuming that the density of O_2 depends only on the altitude, then $N_{O_2} = N_{O_2}(h) = N_{O_2}(h(s'))$ at the point P. The integration $\int_0^s N_{O_2}\sigma_{a\lambda}ds'$ becomes $\int_0^s N_{O_2}(h(s'))\sigma_{a\lambda}ds'$, and can be performed numerically. We estimate O_3 absorption using the expression $\sigma_{a200}/\sigma_{a\lambda} = \ln T_{200}/\ln T_\lambda$, where σ_{a200} is the O_3 absorption cross-section at 200 nm wavelength, T_{200} is the transmittance at 200 nm wavelength calculated using MOSART, and T_λ is the transmittance of interest. This expression can be directly derived from the solution to the Lambert's law, and the absorption cross-sections of O_3 are provided by *Molina and Molina* [1986] and *Burrows et al.* [1999]. We follow similar procedures to calculate molecular Rayleigh scattering by assuming that the scattering cross-section varies $\sim 1/\lambda^4$.

[8] The nominal pointing direction of the ISUAL instrument is 27.5 degrees down from the local horizontal and the field-of-view of the instrument covers a horizontal region of the atmosphere starting at 2000 km from the satellite and extending all the way to the limb at 3106 km along the 60 km altitude layer [*Mende et al.*, 2004a]. Using the altitude (h_r = 891 km) of the FORMOSAT-2 satellite and assuming that the sprite-satellite distance is 2500 km, the transmittance curves for four emission altitudes (h_s = 40, 50, 60, and 70 km) are calculated and shown in Figure 3.

2.3. Intensity Ratios

[9] The streamer model calculates emissions from an individual streamer, but sprites consist of many streamers.

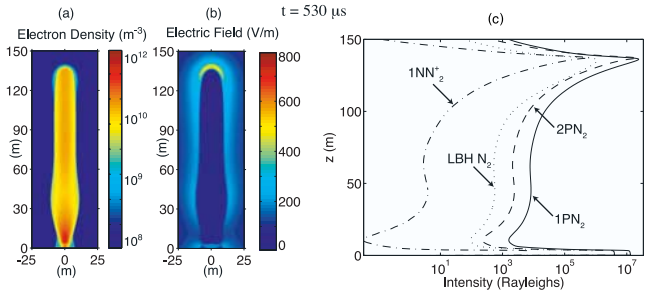

Figure 1. Modeling results on a streamer advancing in a weak electric field at 70 km altitude: (a) electron number density, (b) electric field, and (c) intensity (in Rayleighs) profiles of $1PN_2$, $2PN_2$, $1NN_2^+$ and LBH N_2 emissions along the central axis of the modeled streamer.

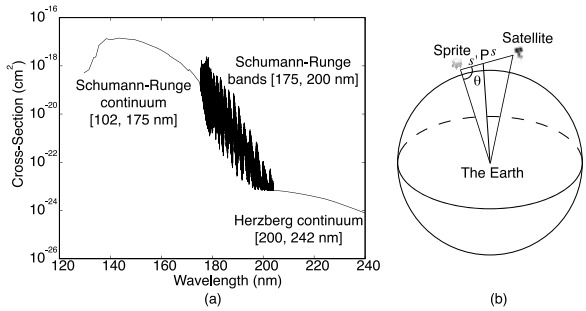

Figure 2. (a) O_2 absorption cross-sections [e.g., *Yoshino et al.*, 1992; *Minschwaner et al.*, 1992; *Amoruso et al.*, 1996; *Yoshino et al.*, 2005]. (b) Observational geometry.

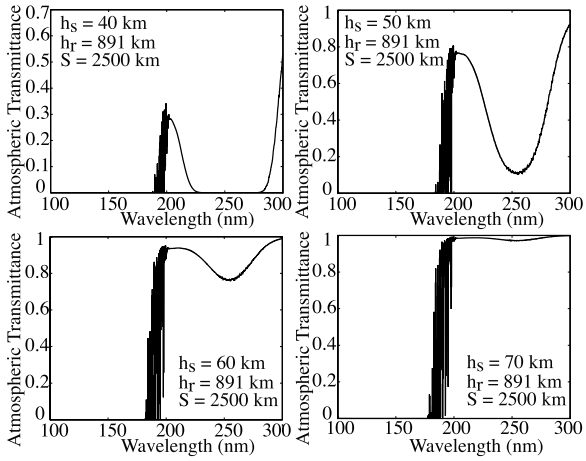

Figure 3. Atmospheric transmittance for four different observation geometries.

If we choose intensity ratios between different band emission systems as our comparison quantity, we expect the ratio for a streamer to be capable to represent the same quantity for a whole sprite. However, the intensity ratios corresponding to the streamer head and the streamer channel are different [*Liu and Pasko*, 2005]. We therefore take the ratios between the total (i.e., integrated over entire streamer body) emission intensity of different emissions. The calculated total emission intensities represent total number of photons emitted per second, and related ratios can be directly compared to similar ratios derived from ISUAL spectrophotometric data.

[10] Streamers at pressures lower than several Torr (i.e., >40 km altitude) hold similarity laws [*Liu and Pasko*, 2004], and sprite streamers at different altitudes driven by approximately the same reduced electric field E/N (N is the gas density) have the same normalized electron energy distribution function $\bar{n}(\varepsilon)$ at a specific location. The electron energy distribution function $n(\varepsilon)$ is usually normalized as $\int_0^\infty n(\varepsilon)d\varepsilon = n_e$, where n_e is the electron number density, and $\bar{n}(\varepsilon)$ is introduced as $\bar{n}(\varepsilon) = n(\varepsilon)/n_e$. Therefore, the ratios of the excitation coefficients for upper states leading to emissions in the four band systems considered in this study are unvarying with altitude for the same reduced electric field, and the altitude variations of the emission intensity ratios are only due to quenching and atmospheric attenuation effects.

[11] Each channel of the ISUAL spectrophotometer detects only a fraction of the band emission, which falls within the photometer filter passband. We ignore the contribution from $1NN_2^+$ and N_2^+ Meinel emission band system to the channel 2 and channel 4, because the intensities of these two emissions are much smaller than $2PN_2$ and $1PN_2$, respectively. We use the data provided by *Mende et al.* [2004a, Table 2] to estimate the fraction of the modeled total emissions of $2PN_2$, $1NN_2^+$, and $1PN_2$ passed by channels 2, 3, and 4, respectively. Therefore, channel 2 records 27.8% of the total emissions of $2PN_2$, channel 3 records 66% of the total emissions of $1NN_2^+$, and channel 4 records 11% of the total emissions of $1PN_2$. For channel 1, we combine the channel filter responsivity profile with the atmosphere transmittance curve for assumed 70 km source altitude (the bottom right panel in Figure 3) to obtain 11% of the total LBH emissions measured by this channel.

3. Results and Discussion

[12] We choose a sprite event reported previously by *Mende et al.* [2004a, 2004b] and *Frey et al.* [2004] to conduct the comparison. The event was observed on July 18, 2004. The lightning occurred at 21:30:15.310 UT, and the sprite started at 21:30:15.316 UT. We could clearly separate the sprite from the lightning signal due to the 6 ms time difference between the occurrence of the lightning and the sprite. To extract the sprite contribution from the photometer data, we first subtract background signal level from the data and then remove lightning contaminations by assuming an exponential decay of the lightning emissions [*Kuo et al.*, 2005]. Figure 4 illustrates the intensity ratios of $2PN_2$ to LBH, $1NN_2^+$ and $1PN_2$ obtained from the streamer modeling results and ISUAL spectrophotometric measurements. The solid lines correspond to the streamer shown in Figure 1. We note that there is an enhancement (Figure 1c) of the emissions near the lower boundary (z = 0 m) of the simulation domain due to the effect of the spherical electrode. However, the change of the three intensity ratios due to this enhancement is less than five percent and does not affect any conclusions derived in this paper. The dashed lines in Figure 4 show the intensity ratios obtained by the ISUAL spectrophotometer with a time resolution of 0.1 ms. We note that the three samples of $2PN_2$ at 316.3 to 316.5 milliseconds (corresponding to 0.4–0.6 ms time interval in Figure 4) saturate the photometer, and the ratios from ISUAL measurements therefore only estimate lower limits at these three moments of time. The three intensity ratios obtained from streamer modeling results and ISUAL spectrophotometric measurements reach the best agreement (within a factor of 2) at the initial development stage of sprites (within 1 ms after the sprite initiation). The $2PN_2$ to $1NN_2^+$ ratio obtained from the streamer modeling is ~55, while it is ~37 according to the ISUAL measurements. The $2PN_2$ to $1PN_2$ ratio is ~0.5 and ~0.2 for the modeling and the ISUAL measurements, respectively. The $2PN_2$ to LBH ratio is ~6.2 and ~8.5 for the modeling and the ISUAL measurements, respectively. We note, however, that the $2PN_2$/LBH ratio is obtained from the streamer model assuming the source altitude 70 km. This ratio is expected to be higher for streamers developing at altitudes <70 km due to quenching (see Table 1 and discussion by *Liu and*

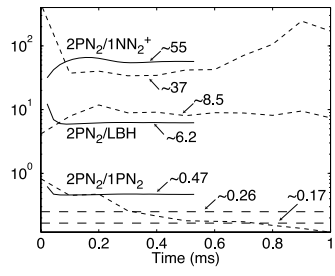

Figure 4. Intensity ratios calculated using modeling results for a streamer shown in Figure 1 (solid line); intensity ratios from ISUAL measurements starting at 315.9 ms (dashed line) (see text).

Pasko [2005]) and atmospheric attenuation (Figure 3) effects on LBH emissions.

[13] Since emissions from sprite streamers in weak electric fields are mostly coming from heads of streamers [*Liu and Pasko*, 2005], we expect that the ratios obtained from the streamer modeling would not vary much after the formation stage. However, as can be seen from Figure 4 at later sprite stage, there is a large difference between the ratios obtained from the modeling and from the ISUAL measurements. The quasi-electrostatic field driving sprite phenomena is expected to change as a function of time, while in the streamer modeling the applied field remains unvarying during the simulation time. Therefore, the reported streamer modeling may not be applicable to interpretation of the experimental data at the later stage of sprite development. Another reason for the observed differences is that sprite signals at this stage are weak, and the operation used in the above analysis to extract the sprite contribution from the ISUAL spectrophotometric data may result in a large relative error.

[14] It is worthwhile to further discuss the ratio of $2PN_2$ to $1NN_2^+$ because of the large difference between their excitation energy thresholds. The fact that the ratio from ISUAL measurements is smaller than the ratio from the streamer modeling (see Figure 4) implies that the maximum electric field driving sprite emissions must be larger than $\sim 3E_k$ (the maximum field at the simulated streamer head shown in Figure 1b). The weak applied field chosen for the streamer modeling in Figure 1 is about one sixth of the conventional breakdown threshold at 70 km altitude. A slight increase in the magnitude of the applied field would lead to an increase in the electric field in the streamer head, leading to a better agreement of streamer modeling and ISUAL measurements.

[15] We note that the electric field magnitudes estimated in the present study ($\geq 3E_k$) are significantly greater than those obtained by *Morrill et al.* [2002] ($\sim 3E_k$), and the difference may be explained by the low temporal resolution of their observations [*Liu and Pasko*, 2005]. Recently, *Kuo et al.* [2005] utilized the $2PN_2/1NN_2^+$ ratio to analyze five sprite events observed by the ISUAL instrument and estimated the upper limit of the electric field driving the sprite emissions to be greater than $3E_k$, in a good agreement with our present study.

[16] **Acknowledgments.** This research was supported by NASA NAG5-11832 and NSF ATM-0134838 grants to Penn State University. Participation of D. H. Burkhardt was supported by NSF EEC0244030 grant to Penn State University.

References

Amoruso, A., L. Crescentini, M. S. Cola, and G. Fiocco (1996), Oxygen absorption cross-section in the Herzberg continuum, *J. Quant. Spectrosc. Radiat. Transfer*, *56*, 145–152.

Burrows, J. P., A. Richter, A. Dehn, B. Deters, S. Hmmelmann, S. Voigt, and J. Orphal (1999), Atmospheric remote-sensing reference data from GOME-2: Temperature-dependent absorption cross sections of O_3 in the 231–794 nm range, *J. Quant. Spectrosc. Radiat. Transfer*, *61*(4), 509–517.

Chern, J. L., R. R. Hsu, H. T. Su, S. B. Mende, H. Fukunishi, Y. Takahashi, and L. C. Lee (2003), Global survey of upper atmospheric transient luminous events on the ROCSAT-2 satellite, *J. Atmos. Sol. Terr. Phys.*, *65*, 647–659, doi:10.1016/S1364-6826(02)00317-6.

Cornette, W. M., P. Acharya, D. Robertson, and G. P. Anderson (1995), Moderate spectral atmospheric radiance and transmittance code (MOSART), *Philips Lab. Tech. Rep. PL-TR-94-2244*, Dir. of Geophys., Hanscom Air Force Base, Mass.

Frey, H., S. Mende, R. R. Hsu, H. T. Su, A. Chen, L. C. Lee, H. Fukunishi, and Y. Takahashi (2004), The spectral signature of transient luminous events (TLE, sprite, elve, halo) as observed by ISUAL, *Eos Trans. AGU*, *85*(47), Fall Meet. Suppl., Abstract AE51A-05.

Gerken, E. A., and U. S. Inan (2002), A survey of streamer and diffuse glow dynamics observed in sprites using telescopic imagery, *J. Geophys. Res.*, *107*(A11), 1344, doi:10.1029/2002JA009248.

Kuo, C. L., R. R. Hsu, H. T. Su, A. B. Chen, L. C. Lee, S. B. Mende, H. U. Frey, H. Fukunishi, and Y. Takahashi (2005), Electric fields and electron energies inferred from the ISUAL recorded sprites, *Geophys. Res. Lett.*, *32*, L19103, doi:10.1029/2005GL023389.

Liu, N., and V. P. Pasko (2004), Effects of photoionization on propagation and branching of positive and negative streamers in sprites, *J. Geophys. Res.*, *109*, A04301, doi:10.1029/2003JA010064.

Liu, N., and V. P. Pasko (2005), Molecular nitrogen LBH band system far-UV emissions of sprite streamers, *Geophys. Res. Lett.*, *32*, L05104, doi:10.1029/2004GL022001.

Marshall, R. A., and U. S. Inan (2005), High-speed telescopic imaging of sprites, *Geophys. Res. Lett.*, *32*, L05804, doi:10.1029/2004GL021988.

Mende, S. B., et al. (2004a), Spacecraft based studies of Transient Luminous Events, paper presented at NATO Advanced Study Institute on Sprites, Elves and Intense Lightning Discharges, NATO, Corte, France, 24–31 July .

Mende, S., H. Frey, R. R. Hsu, H. T. Su, A. Chen, L. C. Lee, H. Fukunishi, and Y. Takahashi (2004b), Sprite imaging results from the ROCSAT-2 ISUAL instrument, *Eos Trans. AGU*, *85*(47), Fall Meet. Suppl., Abstract AE51A-02.

Mende, S. B., H. U. Frey, R. R. Hsu, H. T. Su, A. B. Chen, L. C. Lee, D. D. Sentman, Y. Takahashi, and H. Fukunishi (2005), D region ionization by lightning-induced electromagnetic pulses, *J. Geophys. Res.*, *110*, A11312, doi:10.1029/2005JA011064.

Minschwaner, K., G. P. Anderson, L. A. Hall, and K. Yoshino (1992), Polynomial coefficients for calculating O_2 Schumann-Runge cross sections at 0.5 cm^{-1} resolution, *J. Geophys. Res.*, *97*(D9), 10,103–10,108.

Molina, L. T., and M. J. Molina (1986), Absolute absorption cross sections of ozone in the 185- to 350-nm wavelength range, *J. Geophys. Res.*, *91*(D13), 14,501–14,508.

Morrill, J., et al. (2002), Electron energy and electric field estimates in sprites derived from ionized and neutral N_2 emissions, *Geophys. Res. Lett.*, *29*(10), 1462, doi:10.1029/2001GL014018.

Raizer, Y. P. (1991), *Gas Discharge Physics*, Springer, New York.

Sentman, D. D., E. M. Wescott, D. L. Osborne, D. L. Hampton, and M. J. Heavner (1995), Preliminary results from the Sprites94 campaign: Red sprites, *Geophys. Res. Lett.*, *22*, 1205–1208.

Stanley, M., P. Krehbiel, M. Brook, C. Moore, W. Rison, and B. Abrahams (1999), High speed video of initial sprite development, *Geophys. Res. Lett.*, *26*, 3201–3204.

Vallance-Jones, A. V. (1974), *Aurora*, Springer, New York.

Yoshino, K., J. R. Esmond, A. S. C. Cheung, D. E. Freeman, and W. H. Parkinson (1992), High resolution absorption cross sections in the transmission window region of the Schumann-Runge bands and Herzberg continuum of O_2, *Planet. Space Sci.*, *40*, 185–192.

Yoshino, K., W. H. Parkinson, K. Ito, and T. Matsui (2005), Absolute absorption cross-sections measurements of Schumann-Runge continuum of O_2 at 90 and 295 K, *J. Mol. Spectrosc.*, *229*, 238–243.

D. H. Burkhardt, N. Liu, and V. P. Pasko, CSSL Laboratory, Department of Electrical Engineering, Pennsylvania State University, University Park, PA 16802, USA. (dburkhar@haverford.edu; nul105@psu.edu; vpasko@psu.edu)

A. B. Chen, R.-R. Hsu, L.-C. Lee, and H.-T. Su, Department of Physics, National Cheng Kung University, Tainan 70101, Taiwan. (alfred@phys.ncku.edu.tw; rrhsu@phys.ncku.edu.tw; loulee@narl.org.tw; htsu@phys.ncku.edu.tw)

H. U. Frey and S. B. Mende, Space Sciences Laboratory, University of California, Berkeley, CA 94720, USA. (hfrey@ssl.berkeley.edu; mende@ssl.berkeley.edu)

H. Fukunishi and Y. Takahashi, Department of Geophysics, Tohoku University, Sendai 980-8578, Japan. (fuku@pat.geophys.tohoku.ac.jp; yukihiro@pat.geophys.tohoku.ac.jp)